# High-Speed Access over Copper: Rate Optimization and Signal Construction

Ali Enteshari, Jarir M. Fadlullah, and Mohsen Kavehrad

**This paper focuses on assessment and design of transmission systems for distribution of digital signals over standard Category-7A copper cables at speeds beyond 10 Gbps. The main contribution of this paper is on the technical feasibility and system design for data rates of 40 Gbps and 100 Gbps over copper. Based on capacity analysis and rate optimization algorithms, system parameters are obtained and the design implementation trade-offs are discussed. Our simulation results confirm that with the aid of a decision-feedback equalizer and powerful coding techniques, namely, TCM or LDPC code, 40 Gbps transmission is feasible over 50 m of CAT-7A copper cable. These results also indicate that 100 Gbps transmission can be achieved over 15 m cables.**

**Keywords: 40GBASE-T, single-carrier capacity, SISO, MIMO.**

## I. Introduction

In the commercial market, the extension of fiber into access networks in small businesses and dense metropolitan areas is a new challenge. It has been known for some time that a major bottleneck in delivering multimedia services to computer users is the low-capacity of LANs. With ever-increasing demand for higher capacities, the need for broadband access is transformed from a convenience to a necessity. So far, data communication has been the main driving force behind increased traffic on the communication networks. Applications stemming from a wide range of disciplines, such as high-performance computing, consumer multimedia, teleconferencing, and telemedicine, are just a few examples that require data rates in the gigabits per second range. To keep up with this explosive growth, ultra high-capacity networks were required, and thus optical networks with terabit capacities have dominated the network core. To enable the end user to take full advantage of this core, reliable high-speed LAN access is required. Providing service in a broadband access LAN using a copper cable approach has the advantages of the network being highly-dependable and cost-effective. This will benefit the providers of service over campus settings, such as hospitals, industry compounds, or universities, with facilities spread over several buildings, in that a quick service upgrade could extend new service offerings. Also, within server farms and data centers, short copper connectors are preferable.

After the release of 10GBASE-T, which supports data rates of 10 Gbps up to a distance of 100 meters (for connecting work areas to a telecommunications room), many IEEE members recognized the potential for higher speed and are currently thinking of ways to deliver tens of Gigabits per second over copper cables. The 10GBASE-T standard specifies 10 Gbps data transmission over unshielded and shielded twisted pair

Manuscript received Apr. 30, 2009; accepted July 8, 2009.

This work was supported by Berk Tek-Nexans, New Holland PA, USA.

Ali Enteshari (phone: +1 814 865 0183, email: enteshari@psu.edu), Jarir M. Fadlullah (email: jmf414@psu.edu), and Mohsen Kavehrad (email: mkavehrad@psu.edu) are with the Department of Electrical Engineering, Pennsylvania State University, University Park, PA, USA.

doi:10.4218/etrij.09.0109.0231

  

cables, UTP and STP, respectively [1], [2]. Researchers have started to study the technical feasibility, broad market potential, and economic feasibility of speeds beyond 10 Gbps over copper [3]. In this paper, we evaluate the possibility of 40 Gbps and 100 Gbps data rates (40GBASE-T and 100GBASE-T) over horizontal balanced CAT-7A cables up to a distance of 50 meters. The objective of IEEE 40(100)GBASE-T is to create an application that is capable of transporting data at a rate of 40(100) Gbps over at least 10 meters of copper cable [4]. The cable industry is promoting the use of CAT-7A cable and more convenient CAT-8 cable to support these demanding applications. State-of-the-art digital signal processors (DSP) will be used to cancel impairments in the twisted-pair cable to ensure adequate signal-to-noise ratio (SNR) to achieve a suggested target average bit error rate of $10^{-12}$ at data rates of 40 Gbps and beyond.

This paper is basically the continuation of the work presented in [3]. The feasibility of data rates of 40 Gbps and 100 Gbps transmission over CAT-7A copper wire was investigated in [3]. This assessment was based on single-input single-output (SISO) capacity analysis, assuming crosstalk signals are adequately attenuated by the corresponding cancellers. Moreover, it turns out that in the work presented in [3], the background noise was underestimated which leads to a longer reach mode, that is, 40 Gbps over 100 m. The system model and capacity bounds considered in [3] are followed in this paper, while the derivation of the formulas are presented in greater detail. The main contribution of this paper is the extension of multi-input multi-output (MIMO) capacity analysis and the application of multiuser theory to demonstrate that SISO implementation can perform as well as MIMO implementation, and this is due to a low FEXT level in CAT-7 cables. Also, the theory and implementation of the probability of error minimization method presented in [3] is elaborated in this paper. We have extended this optimization method to the more important scenario where the margin is maximized. We show that these rate optimization methods achieve the same bandwidth as they both try to minimize the gap to capacity. The coding gain of about 5 dB which can be obtained by 4 dimensional trellis coded modulation was considered in [3]. In this paper, we consider a worst case scenario for background noise in which the noise from mixed-signal circuits is assumed to be the dominant noise. In this case, more complex coding schemes are required to achieve higher coding gain. LDPC coded modulation and signal construction is considered in this paper, and a low-complexity coded modulation with 6 dB coding gain is presented.

Throughout the paper, bold face letters ($\boldsymbol{x}$, $\boldsymbol{y}$) denote $q$-dimensional column-vectors (with elements $x_i$, $y_i$). Capital letters (A, B) denote $q \times q$ matrices (with elements $a_{ij}$, $b_{ij}$), and $\mathbf{H}$ and $\mathbf{G}$ denote matrix-valued functions. We will use these notations both for time and frequency domains, and the distinction will be clear from the context without any confusion. Polynomial matrices in this paper refer to polynomial matrices in $z$, or $D$. The $k$-th delay term matrix coefficients of a polynomial matrix $\mathbf{H}(D)$ will be denoted as $\mathrm{H}_k$, and $\mathbf{I}_N$ is the $N \times N$ identity matrix.

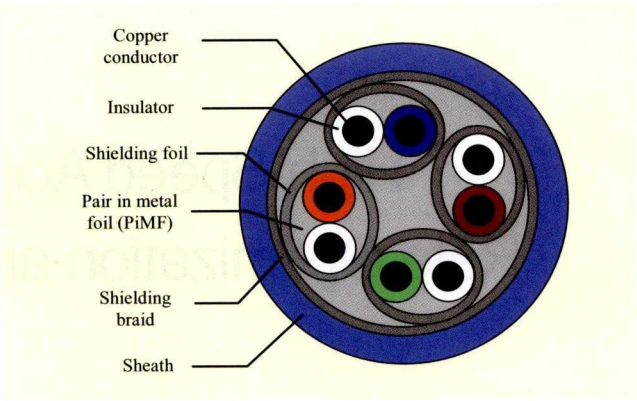


Fig. 1. Cross-section of doubly shielded Category 7 cable.

## II. System Model

Figure 1 shows the CAT-7A cable, which consists of four doubly shielded horizontally balanced copper twisted pairs. The pairs are usually labeled with blue, brown, orange, and green colors. The communication system, therefore, comprises four transceiver pairs on both ends. The matrices signifying channel responses at time $k$T and the corresponding tap-voltage vectors have the following relationship as given in [3]:

$$r_k = \sum_{m=0}^{n_H} \mathrm{H}_m x_{k-m} + \sum_{m=0}^{n_G} \mathrm{G}_m z_{k-m} + v_k \,, \qquad (1)$$

where

- $\boldsymbol{x}_k = [x_k^1, \cdots, x_k^4]$ is the $k$-th sample of vector signal $x(t) = [x^1(t), \cdots, x^4(t)]^{\mathrm{T}}$, which is the input signal to the channel $\mathbf{H}(t)$.
- $\boldsymbol{z}_k = [z_k^1, \cdots, z_k^4]$ is the $k$-th sample of vector signal $z(t) = [z^1(t), \cdots, z^4(t)]^{\mathrm{T}}$, which is the interfering signal from the near-end transmitters.
- $\mathrm{H}_k$=H($k$T) is the discrete matrix impulse response of the vector channel that describes the signal attenuation (insertion loss) and electromagnetic coupling between the twisted pairs (FEXT) [3].
- $\mathrm{G}_k$=G($k$T) is the discrete matrix impulse response of interfering channels representing return loss (RL) and near-end crosstalk (NEXT).

It is assumed that, without loss of generality, all the elements of $\mathbf{H}$ ($\mathbf{G}$) have the same channel order $n_H$ ($n_G$), and

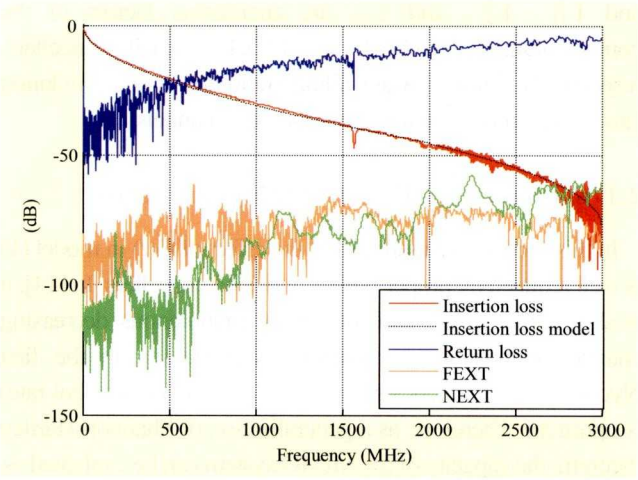


Fig. 2. Insertion loss, return loss, NEXT, and FEXT measurements for 50 m CAT-7A.

$$\mathrm{H}_k=\begin{bmatrix} h_{1,1}(k) & \cdots & h_{1,4}(k) \\ \vdots & \ddots & \vdots \\ h_{4,1}(k) & \cdots & h_{4,4}(k) \end{bmatrix}, \mathrm{G}_k=\begin{bmatrix} g_{1,1}(k) & \cdots & g_{1,4}(k) \\ \vdots & \ddots & \vdots \\ g_{4,1}(k) & \cdots & g_{4,4}(k) \end{bmatrix}.$$

Generally, $x_k$ and $z_k$ share the same statistical properties; they are both zero-mean wide-sense stationary processes, and the 4×4 autocorrelation matrices of $x_k^n$ and $z_k^n$ are given by $\mathbf{R}_{xx}=\mathbf{R}_{zz}=\sigma_s^2\mathbf{I}_4$, which means $x_k^n$ (and $z_k^n$) are uncorrelated, both spatially and temporally with variance $\sigma_s^2$. We also assume that the noise samples are uncorrelated, both temporally and spatially (i.e. $\mathbf{R}_v=\sigma_v^2\mathbf{I}_4$).

Due to the proper shielding of CAT-7A cable, the alien near-end crosstalk is negligible, although if its power is significant, it can be simply included in our model.

Figure 2 shows the insertion loss and return loss measurements of the blue pair ($h_{1,1}$ and $g_{1,1}$) along with the NEXT and FEXT interference signals from the brown pair ($h_{1,2}$ and $g_{1,2}$) as functions of the frequency [3].

Although all our results are based on actual measurements and characterization made by Nexans, for interested readers who want to evaluate/duplicate some of the results, we adopted the following equation which can model the insertion loss of a 50 m CAT-7 cable very well up to 3 GHz ($f$ is in MHz in this equation):

$$\mathrm{IL}_{\mathrm{dB}}=\begin{cases} 0.975\sqrt{f}+0.0025f+0.125/\sqrt{f}, & f\le 2000, \\ -77+\sqrt{3000}-f, & 2000<f\le 3000. \end{cases} \quad (2)$$

## III. Capacity Bounds

### 1. SISO Bounds

In this section, we first review the capacity of the general additive white Gaussian noise (AWGN) channel, and introduce the *single-carrier*, *water-filling*, SISO, and MIMO capacity notations for Category cables.

Before designing mitigation techniques to circumvent channel-induced impairments, the theoretical and practical data transmission capacity limits of the proposed CAT-7A cable must be determined [3]. The channel capacity, $C$, is directly dependent on the physical properties of the medium. The theoretical maximum rate of *error-free* data communication is stated by the Shannon-Hartley theorem [5], [6], which has as parameters a given signal power spectrum, $S(f)$, of an analog communication channel, and the power spectrum, $V(f)$, of possibly colored additive Gaussian noise. According to the theorem, the capacity of a band-limited channel with Gaussian noise is expressed as

$$\begin{aligned} C_{\mathrm{SH}} &= \int_0^W \log_2\left(1+\frac{S(f)}{V(f)}\right)df \\ &\simeq \sum_{n=1}^{N}\frac{W}{N}\log_2\left(1+\frac{S(f_n)}{V(f_n)}\right), \end{aligned} \quad (3)$$

where $C_{\mathrm{SH}}$ is the channel capacity in bits per second, $W$ is the bandwidth of the channel in hertz, and finally, $f$ is frequency in hertz.

An efficient way to utilize the bandwidth of a highly frequency-dispersive communication channel is to divide the available bandwidth into $N$ smaller independent sub-channels, each with nearly flat frequency response. This is possible if $N$ is made large enough [3]. The same reliability can be ensured over all sub-channels by operating them at the same probability of error, $p_e$. Constant $p_e$ can be achieved by using the same class of codes at a constant SNR gap, $\Gamma$, over each channel [7]. The single performance measure that characterizes the multi-channel transmission system in this case is a geometric SNR, which is comparable to the detection SNR of equalized transmission systems [7]. The asymptotic capacity of such a multi-channel transmission system is termed *single-carrier* bound and is given by

$$\begin{aligned} C_{\mathrm{SC}} &= \lim_{N\to\infty} W\sum_{n=1}^{N}\frac{1}{N}\log_2\left(1+\frac{\mathrm{SNR}_n}{\Gamma}\right) \\ &= W\log_2\lim_{N\to\infty}\prod_{n=1}^{N}\left(1+\frac{\mathrm{SNR}_n}{\Gamma}\right)^{\frac{1}{N}}. \end{aligned} \quad (4)$$

The limit can be calculated as

$$\begin{aligned} \lim_{N\to\infty}\prod_{n=1}^{N}\left(1+\frac{\mathrm{SNR}_n}{\Gamma}\right)^{\frac{1}{N}} &= \exp\left(\lim_{N\to\infty}\sum_{n=1}^{N}\ln\left(1+\frac{\mathrm{SNR}_n}{\Gamma}\right)^{\frac{1}{N}}\right) \\ &= \exp\left(\frac{1}{W}\int_0^W \ln\left(1+\frac{\mathrm{SNR}(f)}{\Gamma}\right)df\right). \end{aligned} \quad (5)$$

The single-carrier bound is related to the well-known Salz SNR, which is often used to estimate the system noise margin (required SNR subtracted from achievable SNR) in practical implementations. The Salz SNR is given as in [3] and [8] by

$$\gamma_{\infty}^{W}\{U(f)\} = e^{\frac{1}{W}\int_0^W \ln(U(f))df}, \quad (6)$$

where $U(f) = 1 + \Gamma^{-1}\mathrm{SNR}(f)$. Therefore,

$$C_{\mathrm{SC}} = W \log_2 \gamma_{\infty}^{W}\left(1 + \frac{\mathrm{SNR}(f)}{\Gamma}\right). \quad (7)$$

In fact, this bound indicates the ultimate throughput of a real implementation of a system with finite coding gain and signal processing for any communication medium. Two such implementations are the minimum mean-squared error decision feedback equalizer (MMSE-DFE) [9] and Tomlinson-Harashima precoding (THP) [10], [11].

Given a fixed symbol rate over a set of parallel channels, data rate maximization is obtained by maximizing the achievable $C = \sum_n c_n$ over the average power of each sub-channel, $\mathcal{E}_n$ [3]. The maximization problem can be formulated as in [3] as

$$\lim_{N\to\infty}\left(\underset{\mathcal{E}_n}{\text{maximize}}\ W\sum_{n=1}^{N}\log_2\left(1+\frac{\mathcal{E}_n\left|\mathrm{H}_{kk}(f_n)\right|^2}{\Gamma N_n}\right)\right), \quad (8)$$

$$\text{subject to}\ \sum_{n=1}^{N}\mathcal{E}_n = \sigma_s^2,$$

where $\mathrm{H}_{kk}(f_n)$ represents the transfer function of the $n$-th sub-channel of the $k$-th channel.

We should mention here that the optimization is done separately for each twisted pair. This corresponds to our previous assumption that twisted pairs are more or less similar. One can perform a joint optimization when the characteristics of twisted pairs differ significantly. Lagrange multipliers may be used to obtain optimum parameters for this maximization problem [12]. The corresponding maximum value will henceforth be referred to as the *water-filling* bound, $C_{\mathrm{WF}}$ [13].

For parallel twisted-pair channels, if the individual channels are treated and equalized separately, and the interference signals from other channels are considered as noise (although the power of these interfering signals are attenuated by proper crosstalk cancellers), then the total SISO single-carrier capacity reads as

$$C_{\text{SISO-SC}} = \sum_{k=1}^{4} W \log_2 \gamma_{\infty}^{W}\left(1+\frac{\sigma_s^2\left|\mathrm{H}_{k,k}(f)\right|^2}{\Gamma \mathrm{N}_k(f)}\right), \quad (9)$$

where

$$\mathrm{N}_k(f) = \sigma_v^2 + \sigma_s^2\sum_{\substack{l=1,\\ l\neq k}}^{4}\Gamma_{kl}^{F}\left|\mathrm{H}_{k,l}(f)\right|^2 + \sigma_s^2\sum_{l=1}^{4}\Gamma_{kl}^{N}\left|\mathrm{G}_{k,l}(f)\right|^2,$$

and $\Gamma_{kk}^{N}$, $\Gamma_{kl}^{N}$, and $\Gamma_{kl}^{F}$ are attenuation factors of the corresponding RL, NEXT, and FEXT crosstalk cancellers, respectively. Similar water-filling definition and formulation can be presented for parallel twisted-pair channels.

## 2. Loss between MIMO and SISO Implementations

In this section, we assume that the effect of G($t$) in model (1) is well reduced by proper NEXT and echo cancellers. In [14], it is shown that in the case of strictly monotonous decreasing channel attenuation, a constant power density in the first Nyquist set of frequencies $f \in [-1/2T, 1/2T]$ ($T$: symbol rate) is optimum. Therefore, as a generalization of Shannon-Hartley theorem, the capacity of the MIMO system can be evaluated as

$$C_{\mathrm{MIMO}} = \int_0^W \log_2 det\left(I_4 + \frac{\sigma_s^2}{\sigma_v^2}H(f)H^{\dagger}(f)\right)df, \quad (10)$$

where $W$ is the available bandwidth.

It is quite common, in practice, that in multi-channel systems, individual channels are equalized independently, and crosstalk terms from other channels are removed by fixed or adaptive cancellers. Therefore, the channel matrix $\mathbf{H}$ can be rewritten as

$$\mathbf{H} = \mathbf{D} + \mathbf{F}, \quad (11)$$

where $\mathbf{D}$ and $\mathbf{F}$ are the polynomial matrices containing the diagonal and off-diagonal elements of $\mathbf{H}$, respectively. That is, $\mathbf{D} = diag\{\mathbf{H}_{1,1}, \mathbf{H}_{2,2}, \mathbf{H}_{3,3}, \mathbf{H}_{4,4}\}$ and $\mathbf{F} = \mathbf{H} - \mathbf{D}$.

The decomposition of $\mathbf{H}$ in (11) can be interpreted differently. One can consider this system as a multiple access channel (MAC) with two users as shown in Fig. 3. If the detection starts with user 1, the maximum rate of this user is given as in [11] as

$$C_1 = \int_0^W \log_2 det\left(\mathbf{I}_4 + P(f)\mathbf{D}(f)\mathbf{R}_{nn}^{-1}(f)\mathbf{D}^{\dagger}(f)\right)df, \quad (12)$$

where $\mathbf{R}_{nn} = \sigma_v^2\mathbf{I}_4 + P(f)\mathbf{F}(f)\mathbf{F}^{\dagger}(f)$ and $\int_0^W P(f)df = \sigma_s^2$. Therefore, if the rate of user 1 fulfills $R_1 < C_1$, it can be detected error free and therefore can be removed from the received signal. The remaining signal used by user 2 is now only impaired by the thermal noise, leading to its maximum rate:

$$R_2 = C_2 = \int_0^W \log_2 det\left(\mathbf{I}_4 + \frac{P(f)}{\sigma_v^2}\mathbf{F}(f)\mathbf{F}^{\dagger}(f)\right)df. \quad (13)$$

Recall from multi-user detection theory [15] that $\mathrm{R}_1 + \mathrm{R}_2$ is bounded above by the capacity of the channel, $C_{\mathrm{MIMO}}$. This leads to the conclusion that $\mathrm{R}_1 \le C_{\mathrm{MIMO}} - \mathrm{R}_2$, which means the interference terms must be attenuated enough to achieve high-capacity SISO implementation for user 1. By this method, we can achieve reliable bounds for FEXT attenuation factors, $\Gamma^{\mathrm{F}}$. A similar approach can be used to determine proper attenuation levels for NEXT, $\Gamma^{\mathrm{N}}$.

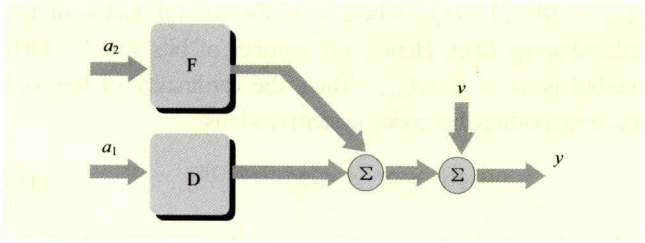


Fig. 3. Decomposition of **H** into diagonal and off-diagonal elements to represent it as a MIMO multiple-access channel.

The preceding analysis is based on MIMO and SISO Shannon capacity bounds. For single-carrier capacities, we can easily replace the corresponding bounds and follow the same analysis. The MIMO single-carrier bound is calculated in the appendix.

## IV. Rate Optimization

In high-speed applications in which the trade-offs of power consumption, implementation complexity, and reliability are dramatically challenging, it is of considerable importance to study the problem of input symbol rate optimization under practical implementation constraints. We obtain the optimum specifications for systems equalized by an ideal (no error propagation) infinite-length minimum mean-squared error–decision feedback equalizer (MMSE-DFE).

### 1. Minimizing the Probability of Error

Here, we are interested in achieving a fixed target bit rate while keeping the probability of error $p_e$ as small as possible. This can be achieved by performance analysis of the coded system and link budget analysis for decision feedback equalizer (DFE) implementation. We assume that the same signal constellation $A$ (that is, M-PAM) is used for each individual channel (dimension). Also, we suppose the power is equally divided among the transmitters. Under these conditions, in CAT-7A cable, it is fairly reasonable to assume the same average error probability for individual channels. The union bound estimate of the probability of symbol decoding error associated with each of these constellations is given as in [16] as

$$p_e \cong K_{\min} Q\left(\sqrt{3\mathrm{SNR}_{\mathrm{norm}} \gamma_c(\Lambda)\gamma_s(\Lambda)/\gamma_m}\right), \qquad (14)$$

where $K_{\min}$ is the multiplicity of codewords with minimum weight, $\gamma_c(\Lambda)$ is the nominal coding gain associated with set partitioning, $\gamma_s(\Lambda)$ is the shaping gain, and $\gamma_m$ is the desired system margin. The $\mathrm{SNR}_{\mathrm{norm}}$ is the normalized SNR and signifies how far a system is operating from the Shannon limit (the *gap to capacity*). More importantly, this quantity is independent of constellation size for large signal spaces [16]. This, in fact, significantly simplifies the underlying analysis. For our QAM baseline, we have $\gamma_s(\Lambda) = 1$ and $\gamma_c(\Lambda) = d^2_{\min}(\Lambda)$. Therefore, $p_e$ reduces to

$$p_e = K_{\min} Q\left(\sqrt{3\mathrm{SNR}_{\mathrm{norm}} \times \frac{d^2_{\min}(\Lambda)}{\gamma_m}}\right). \qquad (15)$$

We should recall that the $\mathrm{SNR}_{\mathrm{norm}}$ defined in this section is the same SNR gap $\Gamma$ used in (7), (8), and (9). From (15), it is clear that $p_e$ is minimized when the $\mathrm{SNR}_{\mathrm{norm}}$ is maximized, assuming that the coding gain and $\gamma_m$ are fixed. We can calculate the $\mathrm{SNR}_{\mathrm{norm}}$ at each frequency from (8) or (9) and substitute into (15) to obtain the error probability versus bandwidth.

### 2. Maximizing the System Margin

Alternatively, the system designer may want to choose a specific reliability level, and seek to maximize the system margin to account for unforeseen sources of performance degradation. By rearranging (15), we can define the systems margin in terms of error probability, coding gain, and gap to capacity as

$$\gamma_m = \frac{3\mathrm{SNR}_{\mathrm{norm}} d^2_{\min}(\Lambda)}{\left(Q^{-1}(p_e / K_{\min})\right)^2}. \qquad (16)$$

This means that, assuming a fixed coding gain, the two optimization scenarios, one that minimizes $p_e$ for fixed $\gamma_m$ and the other that maximizes $\gamma_m$ for a fixed $p_e$, lead to the same optimum bandwidth. In fact, in both cases, $\mathrm{SNR}_{\mathrm{norm}}$ is maximized.

## V. Signal Construction

The previous section revealed the importance of rate optimization to find out the optimum bandwidth and a coding technique that can achieve a given reliability. We can determine a class of coding scheme from the required coding gain and design a proper code. It is known from classic coding theory that a coding gain of up to 5 dB is achievable by trellis-coded modulation at reasonable complexity [17]. A simple but powerful outer Reed-Solomon code can improve this by another 1 dB at the cost of minor bandwidth expansion. Higher coding gain can be obtained by more complex low-density parity-check (LDPC) or turbo codes [18].

Trellis-coded modulation, in spite of its limited coding gain, offers a compact, low-power, low-latency decoding which can be combined with a decision feedback equalizer to eliminate error propagation by replacing the tentative decision with more

reliable ones in the feedback path. This method exploits the survivor path memory of a Viterbi decoder containing the reliable decisions in the feedback path. It is called a *survivor path feedback equalizer* (SPFE) [19]. Malhotra and others extended the SPFE concept for multi-dimensional TCM applicable in multiple channel communications, and also employed soft and hard iterative DFE as more protection against error propagation of DFE [20].

LDPC-assisted coded modulation is adopted for the 10GBASE-T standard [21]. Signal construction is somehow unconventional and is different from the regular set-partitioning rules, but the idea is the same: protect some bits with a good coding scheme and protect the others by maximizing the minimum distance between the constellation points within a coset [17]. We follow the same structure with some modifications and try to generalize the formulations. The goal is to design a high-rate high-gain coding scheme from a low-rate powerful code. Suppose that $g_c$ denotes the minimum required coding gain. An $[\mathcal{N}, \mathcal{K}]$ block code, either systematic or nonsystematic, operating in the *waterfall region* is considered here. We construct the transmit symbols as follows. A block of $\mathcal{K}$ data bits is transformed into $\mathcal{N}$ coded bits, and arranged into a block with $n_r$ rows and $n_c$ columns (If $\mathcal{N} \neq n_r \cdot n_c$ a few dummy bits can be inserted; therefore, we assume $\mathcal{N} = n_r \cdot n_c$ hereafter). Another block of $n_a \cdot n_c$ uncoded bits are stacked with the block of coded bits. Then, every group of $n_a+n_r$ bits, read column wise from the constructed block, is mapped to one constellation point in a two dimensional constellation $\mathcal{X}$, that is, a QAM constellation. The real and imaginary parts of signal points are assigned to two twisted-pairs. The signal points obtained from this constructed block can be assigned to the other two pairs alternately, or another block can be constructed and assigned to the remaining pairs. The results yield a 4-dimensional signal. We denote the cardinality of the QAM constellation as $|\mathcal{X}|$. The total rate of this coding scheme is

$$r_t = \frac{\mathcal{K} + n_a . n_c}{\mathcal{N} + n_a . n_c} > r_C = \frac{\mathcal{K}}{\mathcal{N}}, \tag{17}$$

where $r_C$ is the rate of the original block code.

The signal space $\mathcal{X}$ is partitioned into a number of cosets $\Lambda$ by set partitioning rules, such that $\delta_l^2 \le g_c \le \delta_{l+1}^2$, where $\delta_l^2$ is the minimum intraset distance square at partitioning level $l$. The coded bits are used for coset selection and uncoded bits select the constellation points in each coset. This requires $n_r \ge l+1$ guaranteeing the overall coding gain of $g_c$. To determine $n_a$, assume that a target bit rate of $R_b$ is desired. If a total bandwidth of $W$ is available, the maximum deliverable symbol rate without intersymbol interference is $R_{sym} = 2W/(1+\alpha)$, where $\alpha$ is the roll-off factor of the pulse-shaping filter. Hence, the number of bits sent by each symbol is $n_b = R_b / R_{sym}$. Then, the cardinality of the 4-D space supporting this coded system reads as

$$|\mathcal{X}|^2 \ge 2^{n_b/r_t} = 2^{R_b(1+\alpha)/2Wr_t}. \tag{18}$$

Therefore, if we restrict ourselves to rectangular 2-dimensional lattices, $n_r$ can be determined from $|\mathcal{X}| \ge 2^{n_r+n_a}$. Unfortunately, the parameter $r_t$ in the right-hand side of (3) is implicitly a function of $n_r$. This can be resolved by the following simple algorithm.

Algorithm 1.
1: Initialize $r_t$=0.5;
2: Set $|\mathcal{X}|^2 = 2^{n_b/r_t}$;
3: $n_a = \lfloor \log_2 |\mathcal{X}| - n_r \rfloor$;
4: Update $r_t$ according to the block coded modulation:
$r_t = (\mathcal{K} + n_a \cdot n_c)/(\mathcal{N} + n_a \cdot n_c)$
5: If $n_a \le n_b/(2r_t) - n_r$
exit;
else
$n_a \leftarrow n_a - 1$;
update $r$: $r_t = (\mathcal{K} + n_a \cdot n_c)/(\mathcal{N} + n_a \cdot n_c)$;
end
6: Goto 2

The algorithm starts initializing the total rate with a small rough value. This simply overestimates $n_r$ to make sure that the signal constellation is large enough to accommodate all the $2^{n_b/r_t}$ signal points. Then, the actual rate is calculated according to (2), and an upper bound for $n_a$ is obtained, that is, $n_b/(2r_t) - n_r$. If $n_r$ falls under this constraint, then the algorithm stops; otherwise, $n_r$ is decreased one unit and the rate is updated. This procedure continues until a value of $n_a$ that satisfies all the constraints is obtained.

At the receiver, first the likelihood ratios of coded bits $u_k, k = 1, \cdots, n_r$ are calculated and estimates for the coded bits are obtained:

$$\Lambda_k = \frac{\Pr(u_k = 1 | \boldsymbol{r})}{\Pr(u_k = -1 | \boldsymbol{r})} = \frac{\sum_{\mathbf{u}, u_k = 1} e^{-\frac{1}{2\sigma_v^2}\|\boldsymbol{r} - \mu(\mathbf{u})\|}}{\sum_{\mathbf{u}, u_k = -1} e^{-\frac{1}{2\sigma_v^2}\|\boldsymbol{r} - \mu(\mathbf{u})\|}}, \tag{19}$$

where $k = 1, \cdots, n_r$. Once the estimates $\hat{\boldsymbol{u}}_1$ are provided, the remaining uncoded bits can be estimated by the minimum Euclidean distance rule in coset $\Lambda^{(\hat{u}_1)}$, that is,

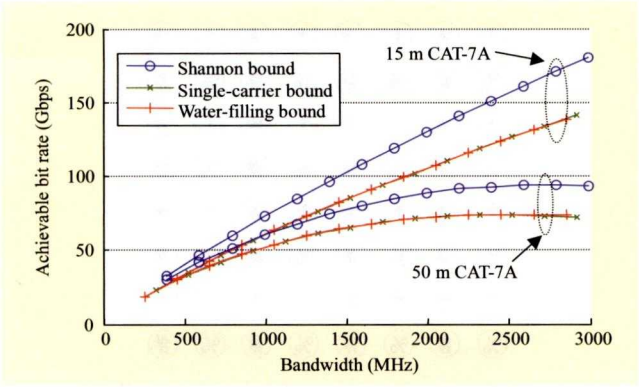


Fig. 4. SISO Shannon, single-carrier, and water-filling capacity bounds.

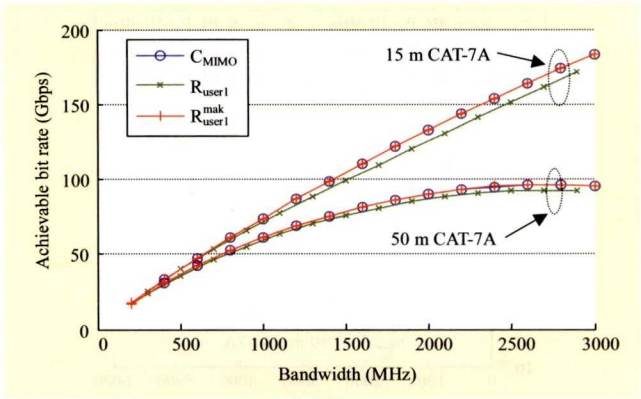


Fig. 5. MIMO capacity and rate $R_1$ for 50 m cable.

Table 1. Parameters for capacity analysis.

| | Tx power (dBm) | Margin (dB) | Probability of error | Coding gain (dB) |
|---|---|---|---|---|
| 15 m | 5 | 0 | $10^{-12}$ | 3 |
| 50 m | 10 | 0 | $10^{-12}$ | 6 |

Table 2. Capacity bounds for 50 m cable and 5 dBm Tx power.

| | Shannon bound | Single-carrier bound | Water-filling bound |
|---|---|---|---|
| $g_c$=6 dB | 79.26 | 60.48 | 60.52 |
| $g_c$=9 dB | 79.26 | 69.11 | 69.18 |

$$\hat{\boldsymbol{u}}_2 = \mu^{-1}\left(\arg\min_{\boldsymbol{x}_n \in \Lambda^{(\hat{\boldsymbol{u}}_1)}} \|\boldsymbol{r} - \boldsymbol{x}_n\|\right), \tag{20}$$

where $\boldsymbol{x} = \mu(\boldsymbol{u}_{n_r+1:n_r+n_a})$ is the labeling function.

## VI. Simulation Results

The SISO single-carrier and water-filling bounds were calculated for 15 m and 50 m CAT-7A cables. Although these cables are much better in terms of isolation and thermal noise compared to other UTP cables, we set the background noise level to -146 dBm/Hz in our simulations [21]. This is mainly because the noise from the analog front-end is dominant in these systems. The capacity bounds and the corresponding optimum bandwidths can be obtained from Fig. 4. The MIMO capacity and user 1 admissible rate were also calculated for these cables and are shown in Fig. 5. The parameters for these simulations are listed in Table 1. Also, echo interference was attenuated by 65 dB while no NEXT or FEXT cancellation was applied.

There are a few observations worth noting regarding Fig. 5. First, for 50 m cable, the maximum data rate of user 1 is only 3 Gbps less than the total MIMO capacity of this channel, which indicates that the amount of information carried by the FEXT channels is negligible. Second, the SISO capacity of this cable has a maximum of 93 Gbps without any FEXT and NEXT cancellation, which is about the same as the maximum rate of user 1. This proves that the channels are isolated from each other very well, and they perform almost as well as isolated parallel channels. Finally, despite the fact that MIMO outperforms the SISO system, it results in a very minor improvement over SISO implementation at a higher cost and power consumption which may not be acceptable.

Some designers may argue about high transmit power and the stresses that it may cause in future submicron CMOS technologies and try to reduce the transmit power at the cost of more complex and sophisticated codes. We repeated the SISO capacity analysis for 50 m cable with 5 dBm transmit power, which causes less non-linearity in the line driver. The capacity bounds obviously drop from their maximum points in Fig. 4. We also repeated this analysis for 9 dB coding gain. To avoid the extra cost of this complex code, one can cut back the cable length by a few meters to keep the code less complex with 6 dB gain. The capacity bounds corresponding to these two codes at 5 dBm transmit power are presented in Table 2. The capacity bound values in this table are in Gbps.

Now, we consider two communication systems transporting data at rates of 40 Gbps and 100 Gbps over 50 m and 15 m, respectively, of horizontal balanced CAT-7A cables. These systems are equalized by an ideal infinite-length MMSE-DFE. Figure 6 shows the variation of $p_e$ as a function of bandwidth $W$ for a target system margin of 0 dB. Other parameters are kept fixed.

The system margins versus bandwidth of these systems are shown in Fig. 7. The system transmitting data at 40 Gbps over 50 m passes the 6 dB margin requirement (Conventionally, a 6 dB margin is considered for multi-gigabit transmission over copper) if a 6 dB coding gain is available around 1.6 GHz. A 3 dB

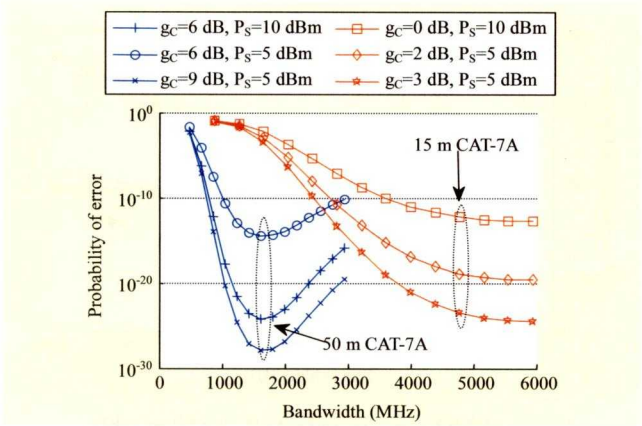


Fig. 6. Minimization of probability of error for 40 and 100GBASE-T systems.

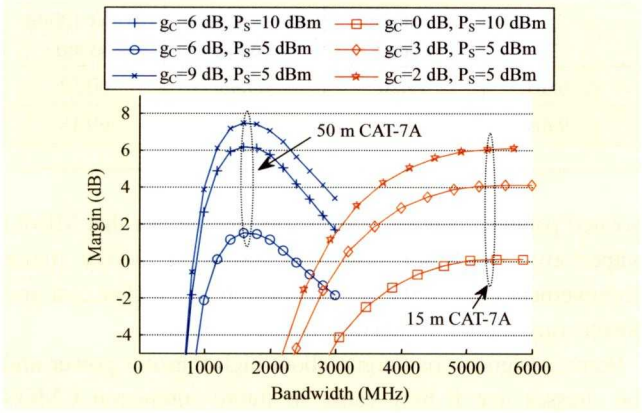


Fig. 7. Maximization of margin for 40 and 100GBASE-T systems.

coding gain for a system transmitting data at 100 Gbps can guarantee the 6 dB margin around 5.5 GHz.

Some observations are worth mentioning here. First, the probability of error minimization and margin maximization occur at the same optimum bandwidth. In general, this bandwidth can be different from the bandwidth obtained under different optimization criteria, such as the power minimizing bandwidth of the MMSE-DFE. Second, Figs. 6 and 7 do not show any symmetry in the optimum bandwidth. More precisely, the optimal bandwidth can generally be overestimated by a few percent rather than under-estimated without any serious degradation. The flatness of curves around the optimum point differs in different scenarios. Finally, it is apparent from Figs. 6 and 7 that the DFE can suffer significant performance degradation when the transmission bandwidth is not optimized. Therefore, for high data rate applications, the process of rate optimization becomes extremely important.

Now we present the simulation results of LDPC-assisted coded modulation for a 40GBASE-T system over 50 m CAT-7A cable. A 6 dB coding gain is required for this system to

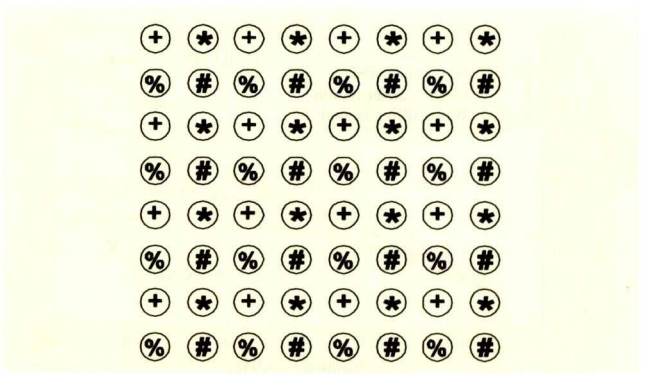

Fig. 8. 6 dB set partitioning on 64-QAM constellation.

Table 3. Number of levels vs. bandwidth for 40 Gbps.

| Bandwidth (MHz) | 1500 | 1550 | 1600 | 1650 | 1700 | 1750 | 1800 |
|---|---|---|---|---|---|---|---|
| M-PAM | 18 | 16 | 15 | 14 | 14 | 13 | 12 |
| Margin (dB) | 6.05 | 6.1 | 6.13 | 6.11 | 6.08 | 6.05 | 6.0 |

achieve the probability of error $10^{-12}$ with a 6 dB system margin. As a demonstration, we used a rate 0.5 (3, 6)-LDPC code with 408 parity check bits and 816 block length. This code was selected from the *Encyclopedia of Sparse Block Codes* by D. MacKay [22]. The 6 dB set partitioning on the 64-QAM constellation is shown in Fig. 8.

Simulations were performed to determine the number of levels in each coordinate in the coded modulated system by varying the signal bandwidth or, correspondingly, the symbol rate. A roll-off factor of 8% was assumed. The results of this simulation are summarized in Table 3. The corresponding system margin at each symbol rate was also calculated and is presented in this table. The resulting bandwidths are for system margins of greater than 6 dB. Among these, the one that achieves a lower number of levels is preferred. However, as the signal bandwidth increases, the design of the mixed-signal circuitry, that is, A/D and D/A becomes more complex and challenging. Furthermore, for the sake of implementation ease, we may prefer the number of levels to be a power of 2.

For this specific example, further simplifications in terms of mapping can be applied by careful labeling. As explained in the previous section, the two coded bits, $u_1$ and $u_2$, determine one of the cosets +, *, %, or #. The remaining 6 uncoded bits select a constellation point from the selected coset. However, if we select cosets % and + when $u_1$=0 and cosets # and * when $u_1$=1 (accordingly, select cosets % and # when $u_2$=0 and cosets + and * when $u_2$=1), the problem of this 2-D set partitioning and coset selection becomes two separate 1-D set partitioning and coset selection. That is, $u_1$ does a 6 dB set partitioning over

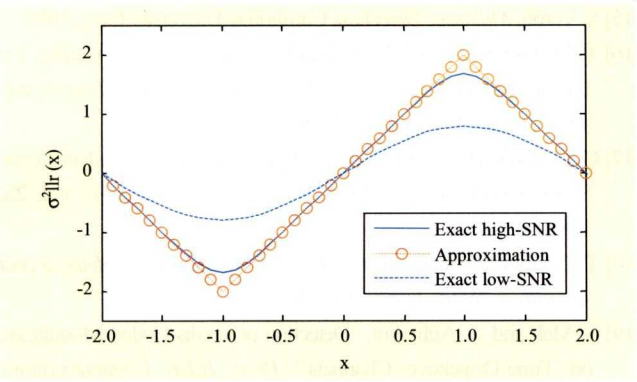


Fig. 9. Scaled LLR value of coded bits.

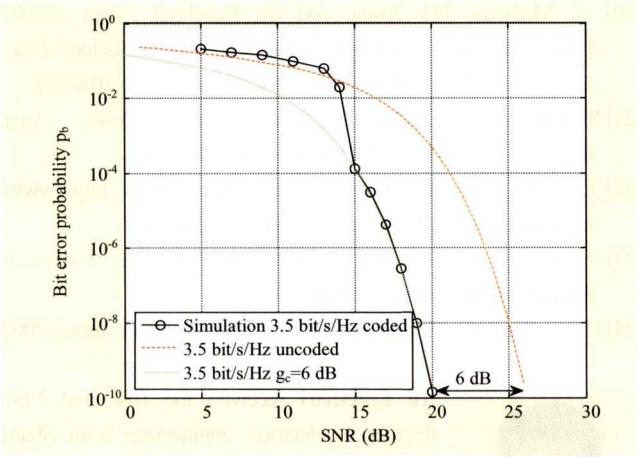


Fig. 10. Bit error probability of coded and uncoded systems.

a real axis on a 16-PAM constellation and $u_2$ does a 6 dB set partitioning over an imaginary axis on the same 16-PAM constellation. The 6 uncoded bits are also divided into two individual groups to select signal points in the selected cosets over real and imaginary axes.

The scaled log-likelihood ratio (LLR) of coded bits as a function of received signal is plotted in Fig. 9 at low and high SNR values. Because this function involves many complex operations, a simplified version of this function can be used:

$$\sigma_v^2 llr(x) \approx \begin{cases} -2x-4, & -2 \le x \le -1 \\ 2x, & -1 \le x \le +1, \\ -2x+4, & +1 \le x \le +2 \end{cases} \quad llr(x) = llr(x+4), \quad (21)$$

where the following approximation is made:

$$\max^*(x, y, \cdots) = \log\left(e^x + e^y + \cdots\right) \approx \max(x, y, \cdots). \quad (22)$$

The results of bit error rate simulation are shown in Fig. 10. At moderately high SNR values, this code achieves a 6 dB gain.

## VII. Conclusion

In this paper, we presented the technical feasibility of high-speed transmission beyond 10 Gbps over standard Category 7A copper wire. Our assessments have revealed that CAT-7A cables are theoretically capable of delivering data streams at a speed of 40 Gbps over 50 m thanks to their excellent shielding and engineering design. Also, based on our modeling and analysis, the maximum achievable rate over 15 m cables is well above 100 Gbps. However, with various degrees of DSP, the goal of running 100GBASE-T over CAT-7A cable can be achieved with some effort by the silicon vendors, probably in the next generations of CMOS technology. We conclude that 40GBASE-T is practical over 50 m of CAT-7A cable, and this is within the realm of expectation of the current objectives of the IEEE standard committee.

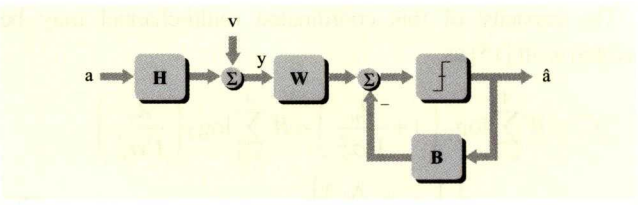


Fig. 11. Block diagram of MIMO MMSE-DFE system.

## Appendix. MIMO Single-Carrier Capacity

The MIMO single-carrier (MIMO-SC) capacity can be bounded by

$$C_{\text{SC}}^{\text{MIMO}} = W \log_2 \left( \frac{1}{\Gamma} \gamma_\infty^W \left\{ det\left( \mathbf{I}_4 + \frac{\sigma_s^2}{\sigma_v^2} \mathbf{H}(f) \mathbf{H}^\dagger(f) \right) \right\} \right). \quad (23)$$

In the following, we show that this bound corresponds to the mean squared error (MSE) minimization of the MIMO-MMSE-DFE system depicted in Fig 11. In this diagram, $\mathbf{W}(z)$ and $\mathbf{B}(z)$ are feedforward and feedback filters, respectively. The estimation error, $\boldsymbol{e}(z)$, is defined as the difference between the input and output variables of the decision-maker device. For optimum filters that minimize the MSE, $\boldsymbol{e}(z)$ is a white sequence [23], that is, $\mathbf{\Phi}_{ee}(z) = \sigma_s^2 \sigma_v^2 \Lambda^{-1}$, where

$$\mathbf{S}_c(z) \triangleq \sigma_s^2 \mathbf{H}^\dagger(1/z^*) \mathbf{H}(z) + \sigma_v^2 \mathbf{I} = \mathbf{Q}^\dagger(1/z^*) \cdot \Lambda \cdot \mathbf{Q}(z).$$

The monic matrix polynomial $\mathbf{Q}(z) = \sum_{m \ge 0} \mathrm{Q}_m z^{-m}$ is causal and minimum-phase, and $\Lambda = diag\{\lambda_1, \cdots, \lambda_4\}$ is a real-valued diagonal matrix. Also, as in [24],

$$\log_2 det\Lambda = \frac{1}{2\pi} \int_0^{2\pi} \log_2 det\left[ \mathbf{S}_c(e^{j\omega}) \right] d\omega. \quad (24)$$

This leads to the signal-to-noise ratio of channel $n$, calculated as

$$\text{SNR}_{\text{MMSE-DFE}}^n = \frac{\sigma_s^2}{\sigma_{e,n}^2} = \frac{\lambda_n}{\sigma_v^2}. \quad (25)$$

The capacity of this coordinated multi-channel may be written as in [15] as

$$C' = W\sum_{n=1}^{4}\log_2\left(1+\frac{\lambda_n}{\Gamma\sigma_v^2}\right) \approx W\sum_{n=1}^{4}\log_2\left(\frac{\lambda_n}{\Gamma\sigma_v^2}\right)$$
$$= W\log_2\left\{\frac{1}{\Gamma}\det\left(\frac{\Lambda}{\sigma_v^2}\right)\right\}, \quad (26)$$

where, in this approximation, we assumed that all the channels are well behaved, that is, $\lambda_n \gg \sigma_v^2, n = 1,\cdots,4$ . This is significantly related to the correct past decisions in the derivation of MIMO-DFE. This reveals that (23) is a lower bound for $C'$, the capacity of coordinated multi-channel system.

## References


[1] Sallaway, *10GBASE-T Channel Criteria*, IEEE 802.3 10GBASE-T Study Group Interim Meeting. Portsmouth, NH, May 21-22, 2003.

[2] M. Kavehrad et al., "10 Gbps Transmission over Standard Category-5 Copper Cable," *Proc. IEEE GLOBECOM'03*, San Francisco, CA, vol. 7, Dec. 2003, pp. 4106-4110.

[3] A. Enteshari and M. Kavehrad, "Transmission Strategies for High-Speed Access over Category-7A Copper Wiring," *IEEE Canadian Conf. Electrical and Computer Engineering, CCECE08*, Niagara Falls, May 2008, pp. 001065-001068.

[4] IEEE 802.3 Higher Speed Study Group Objectives, July 2007.

[5] R.E. Blahut, *Principles and Practice of Information Theory*, Addison-Wesley, 1987.

[6] I. Kalet and S. Shamai, "On the Capacity of a Twisted-Wire Pair: Gaussian Model," *IEEE Trans. Communications*, vol. 38, no. 3, March 1990.

[7] I. Kalet, "Multitone Channel," *IEEE Trans. Communications*, vol. 37, 1989, pp. 119-124.

[8] J. Salz, "Optimum Mean-Squared Decision Feedback Equalization," *Bell System Technical Journal*, vol. 52, Oct. 1973, pp. 1341-1373.

[9] J.M. Cioffi et al., "MMSE Decision-Feedback Equalizers and Coding-Part I: Equalization Results," *IEEE Trans. Communications*, vol. 43, 1995, pp. 2582-2594.

[10] M. Tomlinson, "New Automatic Equalizer Employing Modulo Arithmetic," *Electron. Lett.*, vol. 7, Mar. 1971, pp. 138-139.

[11] H. Harashima and H. Miyakawa, "Matched-Transmission Technique for Channels with Intersymbol Interference," *IEEE Trans. Communications*, vol. 20, 1972, pp. 774-780.

[12] J. Proakis, *Digital Communications*, McGraw-Hill, Aug. 2000.

[13] T.M. Cover and J.A. Thomas, *Elements of Information Theory*, Wiley-Interscience, 1991.

[14] R. Price, "Nonlinear Feedback Equalized PAM Versus Capacity for Noisy Filter Channels," *Proc. IEEE Int. Conf. Communications (ICC)*, Philadelphia, PA, June 1972, pp. 22.12-22.17.

[15] S. Verdú, *Multiuser Detection*, Cambridge University Press, 1998.

[16] G.D. Forney and G. Ungerboeck, "Modulation and Coding for Linear Gaussian Channels," *IEEE Trans. Information Theory*, vol. 44, no. 6, Oct. 1998, pp. 2384-2415.

[17] G. Ungerboeck, "Trellis-Coded Modulation with Redundant Signal Sets-I: Introduction," *IEEE Communications Magazine*, vol. 25, 1987, pp. 5-11.

[18] T.K. Moon, *Error Correction Coding: Mathematical Methods and Algorithms*, Wiley-Interscience, 2005.

[19] S. Mak and A. Aghvami, "Detection of Trellis-Coded Modulation on Time-Dispersive Channels," *Proc. IEEE Communications Theory Mini-Conference*, London, UK, vol. 3, Nov. 1996, pp. 1825-1829.

[20] G. Malhotra, J.H. Jeong, and M. Kavehrad, "Joint MIMO Equalization and Decoding for 10GBASE-T Transmission," *Proc. GLOBECOM'04*, Dallas Texas, vol. 2, Nov. 2004, pp. 918-822.

[21] IEEE P802.3 10GBASE-T Study Group Public Area, http://www.ieee802.org/3/10GBT/public/index.html

[22] D. MacKay, *Encyclopedia of Sparse Block Codes*, http://www.inference.phy.cam.ac.uk/mackay/codes/data.html#l51

[23] S.M. Kay, *Fundamentals of Statistical Processing, Volume I: Estimation Theory*, Prentice Hall, 1993.

[24] H.L.V. Trees, *Optimum Array Processing*, Wiley-Interscience, 2002.



**Ali Enteshari** received the BSc and MSc degrees in electrical engineering from Sharif University of Technology, in 1999, and 2001, respectively. He is currently pursuing the PhD at the Pennsylvania State University, University Park. He was with Signal Co., Tehran, between September 1999 and September 2001 developing signal processing algorithms and designing high-speed circuits. He was a senior engineer in Micro Modje Ind., Tehran, involved in microwave radio design and baseband processing. From 2003 to 2006, he was working on mixed-signal chip design, image sensors, and linear high-efficiency RF amplifiers (LINC). He received the DesignCon'09 Best Paper Award and the Melvin P. Bloom Outstanding Doctoral Research Award, April 2009. His research interests include communications theory, equalization and precoding, coding, multi-input multi-output (MIMO) systems, and OFDM techniques.

**Jarir M. Fadlullah** received the BSEE degree in 2004 from Bangladesh University of Engineering and Technology, Dhaka, Bangladesh. He has been pursuing the PhD in electrical engineering at the Pennsylvania State University, Pennsylvania, since 2005. From 2004 to 2005, he was a lecturer with the Department of Electrical Engineering, Islamic University of Technology, Gazipur, Bangladesh. Currently, he is working with the Center for Information and Communications Technology Research (CICTR) at Penn State. His research interests are multiple-input multiple-output communication system analysis, wireless MIMO channel modeling, and MIMO signal processing. He has experience working with WiMAX systems.

**Mohsen Kavehrad** is with the Pennsylvania State University EE Department as Weiss Chair Professor and director of the Center for Information and Communications Technology Research. He is a fellow of the IEEE and has received 3 Bell Labs awards, the 1990 TRIO Feedback Award for a patent on optical interconnect, the 2001 IEEE VTS Best Paper Award, 3 IEEE LEOS best paper awards and a Canada NSERC PhD-thesis award with his graduate students for contributions to wireless and optical networks. He has over 350 published papers, book chapters, books, and key patents. His research interests are in the areas of wireless and optical communications networked systems.